
MARFA: AN EFFECTIVE LINE-BY-LINE TOOL FOR CALCULATING MOLECULAR ABSORPTION IN PLANETARY ATMOSPHERES

A PREPRINT

Mikhail Razumovskiy *

Moscow Institute of Physics and Technology, Moscow
 mrazumovskyy@gmail.com

Boris Fomin

Central Aerological Observatory, Moscow
 b.fomin@mail.ru

Denis Astanin

Nuclear University MEPhI, Moscow
 densof161922@gmail.com

July 16, 2025

ABSTRACT

We present MARFA (Molecular atmospheric Absorption with Rapid and Flexible Analysis) – an open-source line-by-line tool for calculating absorption coefficients and cross-sections in planetary atmospheres, particularly under conditions of uncertain spectroscopic data and missing continuum functions. With incorporated eleven-grid interpolation technique MARFA shows good performance in computation of far-wing contributions for large line cut-offs. The tool supports flexible parameterization, including line shape functions, wing corrections, user-defined atmospheric profiles, thus, facilitating rapid sensitivity studies for sparse datasets. Spectra are calculated at a high-resolution of about $5 \cdot 10^{-4} \text{ cm}^{-1}$, optimized for infrared and visible spectral regions where HITRAN-formatted line data is available, yet adaptable to other datasets with available line parameters. Output is represented either in a form of binary lookup tables files, directly compatible with radiative transfer codes or in a human-readable format for data analysis and distribution. The MARFA tool is provided in two ways: through a web application accessible at *marfa.app* for onboarding and educational usage, and as an open-source code available in a public repository for advanced utilization, development and contributions.

Keywords molecular absorption · line-by-line modeling · absorption cross-sections · high-resolution spectra · planetary atmospheres · open-source tools

1. Introduction

Since 1960s [1] a significant number of line-by-line Radiative Transfer Models (RTMs) have been developed to model radiative transfer in atmospheres of Earth and other terrestrial planets. Line-by-line approach implies that molecular absorption is treated very accurately by taking into account per-line data. Applications include remote sensing of planetary atmospheres, as well

*Corresponding author

as reference radiative flux calculations necessary for weather and climate modeling. Precise atmospheric absorption calculations are essential in climate and weather studies and in satellite remote sensing of the atmosphere and surface.

One of the most notable models in this domain is the LBLRTM model [2, 3], which is central to the line-by-line methodology and has set standards for next generations of RTMs. In conventional RTMs like LBLRTM, absorption spectra are usually obtained as intermediate values before solving radiative transfer equations. Overall process roughly involves three stages: (1) line-by-line summation of absorption profiles at required atmospheric levels and spectral intervals, (2) incorporation of non-resonant continuum contributions (e.g. collision induced absorption) and optionally convolution with apparatus functions and (3) solving radiative transfer equations to derive radiances, transmittances, fluxes or heating rates. While this workflow is proven to be an effective strategy for Earth-like conditions, environments where continuum function is poorly characterized - as is the case e.g. for Venus [4, 5] - require considering extended line cut-offs. This requirement dramatically increases the costs at stage (1). To target this bottleneck, we have developed MARFA code, which can be understood as a flexible framework for (re-)calculation of molecular atmospheric absorption in data-sparse or uncertain data environments.

MARFA (Molecular atmospheric Absorption with Rapid and Flexible Analysis) is a line-by-line tool optimized for sensitivity analysis of molecular atmospheric absorption, focused on rapid recalculation under uncertain spectroscopic and atmospheric conditions. It is a modern Fortran, open-source code with modular architecture that incorporates an eleven-grid interpolation technique [6] in its core. Application of this interpolation algorithm allows handling large line cut-offs (up to 500 cm^{-1} and beyond if needed) quickly and accurately. MARFA supports flexible parameterization of line shapes, sub-Lorentz corrections, user-defined atmospheric profiles and seamless switching between spectral databases. Its modular design and ability to introduce user-defined features allow users to utilize MARFA as the kernel in their own molecular absorption calculation setups on local computers, without relying on external tools that may not accommodate all use cases (e.g. extreme exoplanetary scenarios). Output values are calculated for all atmospheric levels at once and are provided in a binary pt-format, so afterwards they can directly serve as inputs to radiative transfer codes. The legacy version of MARFA has been tested in remote sensing applications [7], and its efficiency in line-by-line calculations has been independently verified [8].

Particular attention has been given to present codes in a modern and accessible way on the GitHub page, tailored for the scientific and IT communities. The project is well documented in two ways: in-code and outside the code. Within the codebase, we provide extensive comments and clear variable names and their descriptions. Legacy code has very high refactoring coverage making it easier to navigate. Outside the code we provide supporting and comprehensive README file. It includes explanation of installation process and instructions for providing custom features. As with any code project, MARFA is not without areas for optimization and enhancement, but these are transparently listed on the GitHub issues page, providing clarity for anyone interested in working with or contributing to the project. We have placed particular emphasis on organizing MARFA according to best practices of open-source community-driven projects.

As an addition to the MARFA source code which is the main result of this study, we present a web platform marfa.app on which it is possible to interact with a light-weight version of MARFA. On this platform it is possible to perform molecular absorption calculations, generate plots and download data in both binary and human-readable formats. Additionally, it can serve as a valuable educational tool. Though not as rich in functionality as similar platforms (e.g. [9]), it is built on a

modern, highly-scalable programming technologies stack exemplifying the possible direction of future scientific web-based labs. The code for the web platform is also publicly available and can be contributed [10].

The layout of this paper is as follows. In the next section, we explain the physical and computational basis under the core MARFA functionality. It includes brief overview of molecular absorption basis, interpolation technique and discussion of the implemented spectroscopic features. Section 3 provides a specific application scenario for the tool and focuses on the atmosphere of Venus. We show in this section why and how Venus atmosphere is taken as a benchmark. Section 4 discusses the MARFA code design and provides guidance on implementing custom features and outline the tool’s limitation. In subsection 4.6, we provide details on the implementation of the web platform, followed by a few illustrative examples. In Section 5 we give some conclusive remarks and suggestions for future releases.

2. Absorption spectra calculation framework

Considering specifics of calculation of atmospheric absorption in data-sparse environments, our framework prioritizes two main points. Firstly, we aim to equip users with an efficient line-by-line algorithm, minimizing concerns about spectral interval size and line cut-off condition and allowing fast recalculations of spectra on users’ local computers. Secondly, we aim to provide an easily accessible tool by eliminating data hardcoding and to enable smooth parameter input and sensitivity analysis.

2.1. Background

Following the notation by [11], the volume absorption coefficient in the atmosphere can be found by summing the contributions from individual lines across species (l index) and transitions (j index), and then add the continuum function:

$$k_{\nu,\nu} = \sum_{j,l} n^l S_{n,j}^l f_j^l(\nu - \nu_{0,j}^l) + k_{\nu}^c. \quad (1)$$

Our scheme is designed such that a separate calculation is required for each atmospheric species, and the continuum function estimation is not included. Resulting value might be either the volume absorption coefficient k (typically in km^{-1} for atmospheric modeling) or the absorption cross-section σ in $\text{cm}^2/\text{molecule}$, so the expression 1 transforms into:

$$k(\nu; p, T) = n(p, T) \sum_j S_j(T) f_j(\nu - \nu_0; \gamma(p, T)) \quad (2)$$

$$\sigma(\nu; p, T) = \sum_j S_j(T) f_j(\nu - \nu_0; \gamma(p, T)) \quad (3)$$

In expressions 2 and 3 S represents a temperature-dependent line intensity, while f is a normalized line shape function, which depends on both temperature and pressure through the half-width at half-maximum (HWHM) γ . The parameter ν_0 is a center of the line (wavenumber of a transition). The number density n of the species can be determined, for example, from the atmospheric profile and the species’ abundance (usually in ppm). Since the number density n in expression 2 is outside the sum, the program can simply switch between calculation of absorption coefficient 2 and cross-section 3. Initial per-line spectroscopic data, normally taken from spectroscopic databases like

HITRAN [12, 13], HITEMP [14] or GEISA [15, 16], is required to determine entities under the summation sign in expressions 2 and 3.

2.2. Predefined line shapes

Within MARFA we have implemented the Lorentz, Gaussian and Voigt profiles which correspond to pressure-broadening, Doppler broadening and the combination of both effects respectively. Since the primary goal is a calculation of atmospheric absorption, Voigt line shape is set as a default choice. Details of our programmatic implementation of the Voigt function can be found below and in Appendix C.

Predefined Lorentz and Gaussian lines shapes are implemented exactly as per the well-known formulas:

$$f_L(\nu; \gamma_L) = \frac{1}{\pi \gamma_L^2 + (\nu - \tilde{\nu}_0)^2} \quad (4)$$

$$f_G(\nu; \alpha_D) = \sqrt{\frac{\ln 2}{\pi \alpha_D^2}} \exp\left(-\frac{(\nu - \nu_0)^2 \ln 2}{\alpha_D^2}\right), \quad (5)$$

where $\gamma_L = \gamma_L(P, T)$ and $\alpha_D = \alpha_D(T)$ are the corresponding line half-widths and $\tilde{\nu}_0$ is a pressure-shifted line center position.

Voigt line shape is described by the convolutional integral of Lorentzian and Gaussian line shapes:

$$f_V(\nu - \nu_0, \gamma_L, \alpha_D) = f_L \otimes f_G = \int_{-\infty}^{\infty} d\nu' f_L(\nu - \nu', \gamma_L) \times f_G(\nu' - \nu_0, \alpha_D) \quad (6)$$

It can be effectively represented using the Voigt function $K(x, y)$ [17]:

$$f_V(\nu - \nu_0; \gamma_L, \alpha_D) = \frac{\sqrt{\ln 2 / \pi}}{\alpha_D} K(x, y), \quad (7)$$

$$K(x, y) = \frac{y}{\pi} \int_{-\infty}^{\infty} \frac{e^{-t^2}}{(x - t)^2 + y^2} dt, \quad (8)$$

where $x = \frac{\sqrt{\ln 2}(\nu - \nu_0)}{\alpha_D}$ and $y = \frac{\sqrt{\ln 2} \gamma_L}{\alpha_D}$.

Many studies have proposed routines for determining the Voigt function through various numerical expansions, mainly due to its close relation to the complex error function. MARFA builds on the implementation of the Humlíček [18] algorithm, optimized by Kuntz [19] by reducing the number of floating-point operations by considering only the real part of the rational approximation. Additionally, since the primary use case for MARFA is extended line wings, we found it convenient to exploit the asymptotic convergence of Voigt to Lorentz for large x . We have ensured that the errors introduced by these asymptotic substitutions remain below 1%. For more details, please refer to Appendix C. The legacy version of this approach has been successfully adopted in several RTMs and has been highlighted in radiation codes intercomparison research [20, 21]. Our implementation of the Voigt function does not compete for peak precision, but it is efficient and perfectly suitable for setups with large line cut-offs. It should be noted that our focus is not on achieving the highest accuracy in out-of-the-box line shapes but rather on equipping users with the flexibility to introduce their own.

A user can manually introduce custom line shape function by creating a dedicated Fortran function (see documentation [22] for more details). In expressions 2 and 3, the line shape function f_j is always multiplied by the intensity S_j . To ensure compatibility, custom line shapes should follow this combined structure $S_j \times f_j$ inside their Fortran function implementations. For example, one needs to include the function at the end of the `Shapes.f90` module:

```
real function myLineShape(X)
  real(kind=DP), intent(in) :: X ! Distance from line center [cm-1] in double precision
  real :: myLineShape
  ! ... User-defined line shape logic
  myLineShape = myLineShape * intensityOfT(temperature) ! Mandatory  $S_j(T)$  scaling
end function myLineShape
```

and redirect the module's shape function pointer:

```
shapeFuncPtr => myLineShape
```

`IntensityOfT`, implemented in the `Spectroscopy.f90` module, calculates the temperature-dependent line intensity using HITRAN's formulations [23]. Potentially, it can be also substituted with user's defined line intensity function. This design allows custom integration of advanced line profiles (e.g. Tran, Ngo, and Hartmann [24], Ngo et al. [25], Rosenkranz [26], and Varghese and Hanson [27]), without disrupting the main program workflow. Users can easily switch between different line shapes just by `shapeFuncPtr` pointer redirection.

The `Spectroscopy.f90` and `Shapes.f90` modules serve different roles. `Shapes.f90` contains available line shapes functions and governs default line shape selection. It must be noted that the choice of the line shape can significantly affect performance. The `Spectroscopy.f90` module contains standardized routines for calculation of temperature- and pressure- dependent parameters: Lorentz (γ_L) and Doppler (α_D) half-widths, line intensities $S(T)$ and pressure-induced shifts $\tilde{\nu}_0$ following HITRAN's formulations [23]. Both of the modules are opened for extensibility: by users adding custom functionality and by future MARFA releases.

2.3. χ -factors

Experimental data suggest that the far wings of spectral lines deviate from Lorentz or Voigt behavior. To address this, usually so-called χ -correction functions [28, 29] are introduced:

$$f_{\text{corrected}}(\nu - \nu_0) = f_L(\nu - \nu_0)\chi(\nu - \nu_0), \quad (9)$$

The χ -factor is an empirical function typically tied to a specific molecule, and the underlying physical mechanisms governing its absorption behavior. Applying such a correction improves physical reliability and accuracy of the results without compromising performance, because it doesn't require direct computations of underlying mechanisms (e.g. line mixing or finite duration of collisions). Depending on the molecule and specific atmospheric conditions, spectral line wings can exhibit either sub-Lorentzian behavior (e.g., CO₂ [28]) or super-Lorentzian behavior (e.g., H₂O [30]). For example, Tonkov correction [31] to the Lorentzian shape f_L is implemented according to the piece-wise correction function:

$$\chi_{\text{Tonkov}} = \begin{cases} 1.084 \exp(-0.027 |\nu - \nu_0|) & \text{if } 3 \text{ cm}^{-1} \leq |\nu - \nu_0| \leq 150 \text{ cm}^{-1}, \\ 0.208 \exp(-0.016 |\nu - \nu_0|) & \text{if } 150 \text{ cm}^{-1} < |\nu - \nu_0| \leq 300 \text{ cm}^{-1}, \\ 0.025 \exp(-0.009 |\nu - \nu_0|) & \text{if } |\nu - \nu_0| > 300 \text{ cm}^{-1}, \\ 1 & \text{otherwise.} \end{cases} \quad (10)$$

Since we used Venus for benchmark studies (see Section 3. for more details), we have implemented within MARFA several χ -factors for CO₂ line shapes relevant to Venus atmospheric absorption modeling: Tonkov et al. [31], Perrin and Hartmann [32], Pollack et al. [29]. Similar to the Shapes.f90 module, ChiFactors.f90 module contains implemented χ -corrections. It is advisable to add custom-defined functions at the end of this module. Below is an example for users, how to add their own wings corrections functions by interacting with the MARFA codebase, ChiFactors.f90 module:

```
pure function myChiFunction(X, moleculeIntCode) result(myChiFactor)
  implicit none
  real :: myChiFactor
  real(kind=DP), intent(in) :: X ! Distance from line center [cm-1] in double precision
  integer, intent(in) :: moleculeIntCode ! e.g. 1 - H2O, 2 - CO2, ...
  myChiFactor = 1. ! default value

  ! set the molecule int code limitation
  if (moleculeIntCode == 2) then
    !  $\chi$ -factor correction logic here
  end if
end function myChiFunction
```

By default, the shapeFuncPtr pointer directs to the noneChi function, meaning no correction applied. To change that, just redirect the module's χ -function pointer:

```
shapeFuncPtr => myChi
```

MARFA documentation [22] provides additional instructions on how to manually add custom χ -corrections.

2.4. Interpolation technique for the line-by-line modeling

Apart from improved algorithmic approaches for the Voigt function, interpolation techniques are essential for speeding-up line-by-line modeling. Notable works in this domain are: Clough, Kneizys, and Davies [30], Edwards [33], West, Crisp, and Chen [34], Gordley, Marshall, and Chu [35], Sparks [36], Fomin [6], Titov and Haus [37], Kuntz and Höpfner [8], Kruglanski and De Maziere [38], and Schreier [39]. One effective technique for addressing this is the so-called multi-grid approach. It makes estimations of a line profile function on a sequence of grids with increasing step sizes. The concept behind these algorithm is straightforward: moving away from the center of a spectral line results in the profile becoming progressively smoother, as in the case of a Lorentzian wing, where the profile follows $\sim 1/(\nu - \nu_0)^2$. The line profile is divided into sections corresponding to the number of grids. On the finest grid, the central, sharpest parts of the lines are summed. On the next, coarser grid, the smoother parts adjacent to the center are summed, and so on. Once all the parts of the lines have been summed on their respective grids, the discrete functions obtained on these grids are interpolated onto the finest grid, resulting in the desired spectrum.

In MARFA we use a multi-grid interpolation technique described by Fomin [6], which is considered fast and suitable for calculations with various line contour models [8]. We have confirmed that in presence of large line cut-offs, 2 or 3 grids may not be enough to achieve the desired balance between speed and accuracy. To address this, our scheme employs 11 grids with increasing resolution. Interpolation technique is performed on 10 cm⁻¹-length intervals. Number of points in the finest grid is set to $N = 20481$ leading to a resolution of $10/(N-1) \approx 4.88 \cdot 10^{-4}$ cm⁻¹. This is usually sufficient to resolve typical Doppler lines in upper atmosphere in IR-region. The

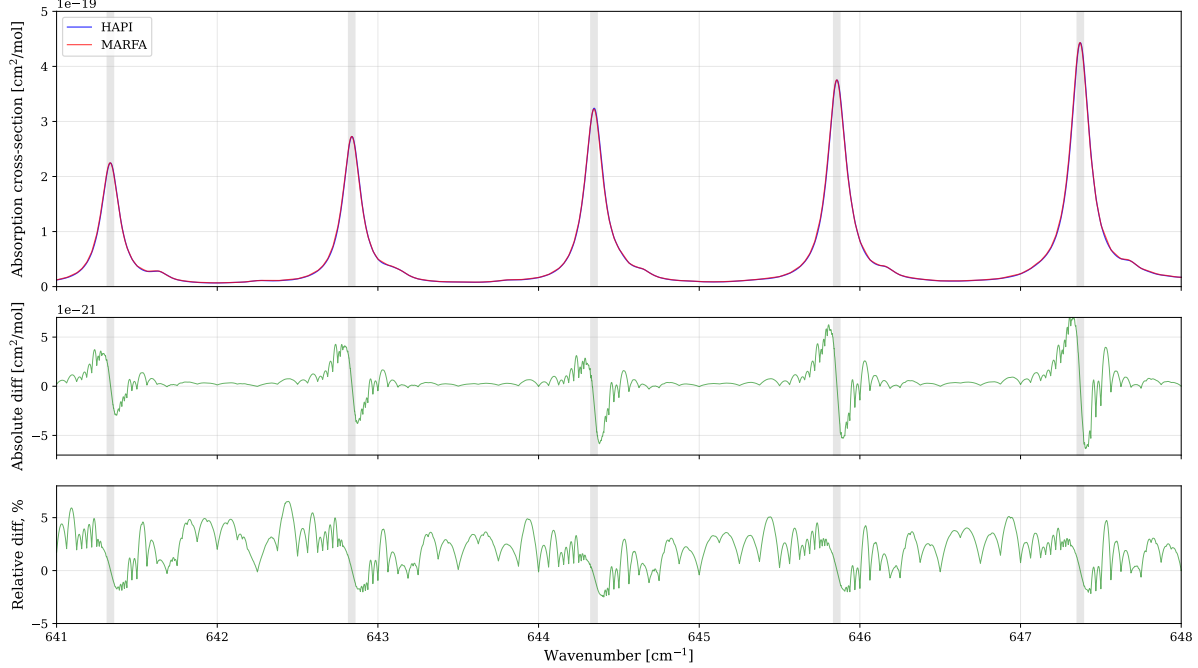


Figure 1: CO₂ absorption cross-sections calculated with HAPI and MARFA under conditions: $P = 1$ atm, $T = 296$ K, Lorentz line profile, 25 cm^{-1} line cut-off and air as a broadening gas

number of points in other grids follow a rule: $N_i = 10 \cdot 2^{i-1} + 1$, $i = 1, 10$ which by our experience is sufficient to describe distant line wings with line cut offs up to 500 cm^{-1} and beyond. Important fact is that the interpolation requires significantly less computational time compared to calculation of line profiles on each grid. Interpolations between coarse and fine grids are performed only once (per subinterval 10 cm^{-1} step) and are independent of the number of lines, making the computation time for spectra logarithmically dependent on the line's half-width. The technique and its accuracy characteristics are detailed in Fomin [6] original study, which also discusses utilization of 3-point and 5-point interpolations in molecular spectra calculations.

To demonstrate speed and accuracy characteristics of MARFA, which in current version employs 3-point interpolations, we performed series of program runs to compare cross-sections computed with MARFA and with HAPI [40] Python library. An example comparison for CO₂ is illustrated on fig. 1. HAPI is known for its seamless integration with HITRAN data and proven reliability of results. When running calculations with HAPI we selected a default equidistant wavenumber grid, avoiding reliance on interpolation techniques, which inherently introduce numerical errors. Spectral resolution in both calculations was kept the same $\sim 5 \cdot 10^{-4}\text{ cm}^{-1}$. For the pressure of 1 atm this resolution is excessive but it gave us opportunity to estimate computational times for the most time-consuming spectra in the upper atmosphere. We found out that MARFA's computation is faster at around 2 orders of magnitude. In the line centers the discrepancies appear to be less than 1%. However, the relative errors shown on fig. 1 in cross-section calculations between spectral lines can reach 5%. These errors can be reduced by an order of magnitude through the use of 5-point interpolation schemes instead of 3-point ones, with only a twofold decrease in computational speed [6]. But as seen from fig. 1, the errors are oscillatory and, as practice shows, tend to cancel out each other to a large extent when integrated over the wavenumber. This case is relevant in the computation of integrated radiative fluxes or in the convolution of spectra with

instrumental functions in remote sensing applications. These types of problems are that MARFA is primarily designed to address. Reference [6] further shows that the integration errors over the line profiles correspond to uncertainties in the line intensity parameter S which at minimum is of 1%. For these reasons, the current version of MARFA keeps the 3-point interpolation scheme.

MARFA currently support a more limited set of spectroscopic options and line shapes compared to HAPI and does not offer direct integration of HITRAN data. However, it provides several advantages. These include: significantly higher calculation speed, support of calculation of absorption coefficients at all atmospheric levels at once, and enhanced functionality for accounting line wings contributions. Since primary aim of MARFA development was to target atmospheric studies for terrestrial planets, and not for purely spectroscopic purposes in Earth' environment, we view these two tools as complementary.

3. Venus as a benchmark scenario

3.1. Why Venus ?

The idea of developing a separate tool for calculating molecular spectra originated during our ongoing work on constructing k-distribution parameterizations suitable for Venus GCMs [41], and particularly in the IR and visible spectral intervals (in progress). During this research, we faced considerable uncertainties in Venus' spectroscopic and atmospheric parameters to provide as inputs for forward radiative transfer model. That led to a need of rapidly recalculating absorption spectra for testing, validating and sensitivity analysis purposes. In Section 3.2., we provide a brief overview of the key uncertainties in the Venus' data essential for obtaining reliable outcomes from radiative transfer models.

In our view, Venus is a good starting point for validation and testing of new, general purpose line-by-line models, which aim to follow a data-driven and flexible approach. Despite decades of ground-based and spacecraft observations that yield substantial information on Venus, when it comes to radiative transfer modeling, reliable atmospheric and spectroscopic data to serve as inputs to forward models, remain limited. As RTMs are highly sensitive to atmospheric and spectroscopic parameters [5], it is important that these models treat such data strictly as inputs, rather than hardcoding them. This is one of the major drawbacks why many Earth-based or data-specific models struggle to accurately capture Venusian conditions.

Venus' unique rotation characteristics and its location within the habitable zone provide a clear analogy to a telluric exoplanet [42, 43]. This makes it a promising test case for validating exoplanetary radiative transfer models. In exoplanetary research, radiative transfer models are highly sensitive to the input molecular absorption data. MARFA addresses this need by providing molecular spectra flexibly and precisely.

3.2. Challenges and uncertainties in Venus atmosphere modeling

For each atmospheric constituent of interest, pre-calculated absorption coefficients are prepared for a set of pressure-temperature (P-T) value pairs. Significant differences in thermal structure with respect to latitude and local time (solar longitude) are observed in models of Venus's middle atmosphere [44, 45]. Temperature profiles in the upper atmosphere differ drastically between the day- and night-side hemispheres [46, 47, 48]. The temperature structure of the lower atmosphere is not well-studied and is often assumed to be homogeneous across the planet (globally averaged) in

models. Due to this reason, interpolation and averaging procedures are employed and that leads to multiple approaches for compiling an a priori initial temperature profile for retrieval procedures [49, 50]. MARFA enables seamless switching between input atmospheric profiles (with up to 200 levels each), rather than just P-T values like conventional methods. It is useful when handling multiple atmospheric profile files and conducting comparative analyses. Radiative heating and cooling rates are usually calculated up to a height of 150 km [5]. This means that constituents mixing ratio profiles should also extend to this altitude. Most models use data compiled from various sources and if lacking data, interpolate to constant values in the upper atmosphere [51, 29, 5].

The selected database for line parameters greatly affects the absorption cross-section and the resulting radiance spectra. Unfortunately, there is no dedicated Venus database with line parameters for all relevant species that accounts for CO₂ broadening and high-temperature conditions. As a result, line parameters for Venus modeling are typically taken from various databases and dedicated experimental studies [4, 50, 5]. Commonly used databases include HITRAN [52, 53, 54, 13, 12], HITEMP [55, 14], CDSD [56], and specific CO₂ data from HITEMP-VENUS [29]. It is important to note that the hot lower atmosphere of Venus presents an additional computational challenge because the use of HITEMP or HITEMP-VENUS databases is generally required over HITRAN. This results in an increase of spectral lines by two orders of magnitude for CO₂ absorption modeling [4]. MARFA's line-by-line scheme shows capability of handling extensive line lists, like HITEMP, what we successfully employed for Venus studies.

Infrared continuum absorption parameters have only been established in specific transparency windows [57, 58, 59, 60], thus leaving the continuum function unavailable for broader spectral intervals in radiative transfer modeling. As a result, contributions from distant line wings must be accounted for. Various χ -factors have been tested to describe the CO₂ sub-Lorentz behavior of spectral lines under Venusian conditions [28, 61, 62, 32, 29, 31, 63], as well as different line cut conditions, typically ranging from 125 to 500 cm⁻¹ [4, 50, 5]. While using MARFA we systematically analyzed impact of these χ -factors and line cut-offs on CO₂ absorption cross sections especially in Venus lower atmosphere. This explains benefits of using MARFA in sensitivity studies of Venus radiative transfer under varying spectroscopic settings.

On the fig. 2 we present monochromatic absorption cross-sections of CO₂ at Venus surface calculated with MARFA for several line cut-off conditions and χ -factors (Tonkov et al. [31], Perrin and Hartmann [32], and Pollack et al. [29]). The blue line represents default Voigt profile, meaning no line wing correction is applied. The fig. 2 is validated against the fig. 10 in Haus and Arnold [4], and shows good fits. Some discrepancies could be found in areas of low absorption most likely due to the choice of different spectral database and spectral resolution. These spectra are generated in high-resolution of $5 \cdot 10^{-4}$ cm⁻¹ and are based on HITRAN2020 line data [12]. In the sensitivity study by Haus, Kappel, and Arnold [5] it has been confirmed that the choice of spectral line database (the most important), sub-Lorentz corrections and line cutoffs are essential for accurate Venus radiative balance modeling. Employing MARFA code allows to generalize this approach, enabling systematic exploration of databases/line shapes/cutoff impacts across diverse conditions.

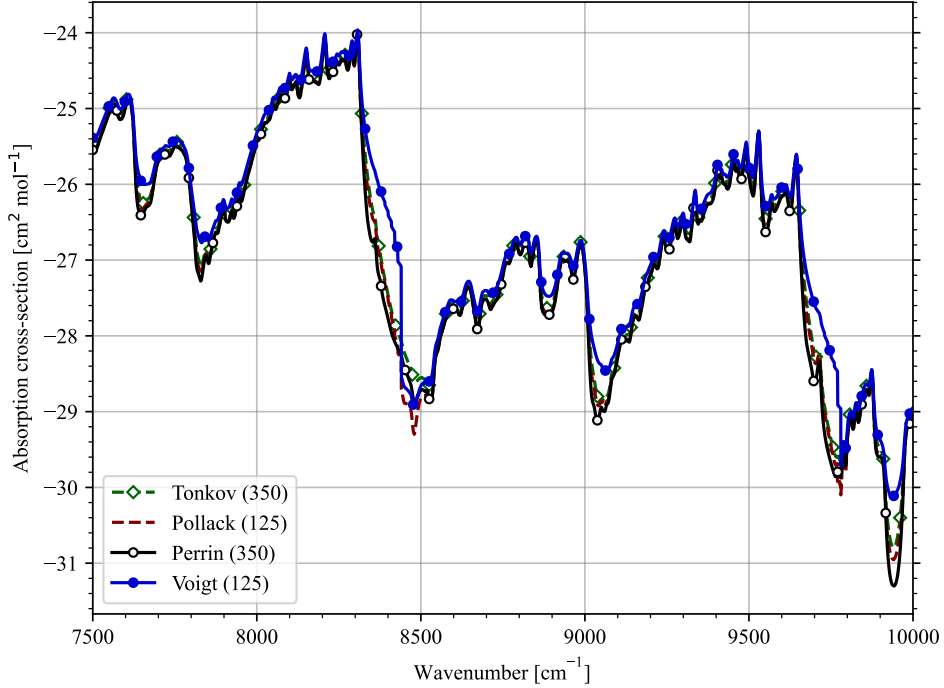


Figure 2: Monochromatic absorption cross-sections of CO_2 at 92.1 bar and 735.3 K as a function of wavenumber in dependence on sub-Lorentzian profile and line-cut condition. Continuum absorption is neglected.

4. Implementation

4.1. Code and project design

In developing MARFA, we address the need for more flexible, data-driven, and efficient general-purpose line-by-line tools. However, specific attention is given to facilitate codes utilization: by both researchers (who just need to run the code) and by developers (who need also to contribute to the code). Scientific codes are known to be poorly adapted for community development, because of their complexity, lack of support, inconsistent coding standards and unrefactored legacy components. Such codes, even if being efficient in algorithmic terms, after distribution are considered often considered as black boxes, complicating the introduction of even small changes. In regard of targeting this issue, we highlight recently released codes for calculating atmospheric absorption by Korkin et al. [64]. The authors of this study follow the so-called “paper-and-code” paradigm, when the paper extensively explains the code, and the code is openly available to complement the paper. Paper gives instructions not only how to run, but also how to change and develop the code. Our approach is closely aligned with this paradigm, although we moved more specific details to the well-structured documentation on the repository home page. Overall, MARFA might be understood as a kernel (or framework), which contains line-by-line scheme, basic line shapes, far wings correction functions and line intensity functions. This kernel is designed to be extensible and reusable under various atmospheric and spectroscopic conditions.

The MARFA project is thoroughly documented to provide quick-start instructions, detailed I/O formats and performance benchmarks [22]. The codebase employs intuitive variable names.

Building and running the source code is straightforward using fpm (Fortran Package Manager) [65]. MARFA is designed through the Fortran modular structure. It means that each module within the source code is dedicated to specific physical or algorithmic operation, such as calculating line shapes, χ -factors, grid calculations, etc. This division to modules improves clarity of the code and allows during development to focus on individual components without a risk affecting the entire program. During development and refactoring of the legacy code, we aimed to avoid using outdated features from older versions and followed the recent Fortran 2023 standard [66, 67]. Although the module `LineGridCalc.f90`, containing implementation of the multi-grid interpolation algorithm, still has legacy features, it does not compromise the overall clarity and maintainability of the code.

Following the surge in popularity of Python within the scientific community, several Python packages have been developed to calculate absorption spectra, either independently or as part of radiative transfer modeling schemes. Studies show (e.g. Schreier [68]) that NumPy library [69] provides comparable efficiency to Fortran or C/C++ languages. Notable examples include HAPI [40], py4Cats [70] (a Python reimplementation of GARLIC [71]), PyRTlib [72], among others. Nevertheless, Fortran was chosen as a main programming language of MARFA, primarily due to the existence of initial legacy code written in that language. Our approach offers two modes of interaction: through the well-documented Fortran source code and via the web platform `marfa.app` which allows users to perform calculations directly by interacting with a lightweight version of the kernel. We may still later consider to convert MARFA or some of its modules (e.g. `LineGridCalc.f90` which contains implementation of the multi-grid algorithm) into a Python package even more facilitating development and distribution.

4.2. Used data

The tool is designed to minimize the amount of data stored within the project directory, with even fewer datasets embedded directly in the source code. Below we provide details about the datasets used in the project.

4.2.1. Spectral Databases

The line-by-line approach implies accessing line data from spectral database files during runtime. For cross-section calculations (or absorption coefficients), only the essential (“core”) line parameters are necessary (see, e.g., Schreier et al. [70]). To enhance efficiency, the MARFA executable expects these parameters to be stored in a binary file with a specified format. The source code offers built-in functionality to convert standard `.par` files into a required binary format. For more details, please refer to the project documentation [22].

Spectral databases for the first 12 molecules (based on HITRAN ID), precalculated to the needed format, are available in the `data/databases/` directory. These files are generated from `.par` files from HITRAN 2020. These files can be used to perform instant calculations or testing. They cover the range from 10 cm^{-1} . By knowing the required file format (see appendix 5.), users can generate and store their own spectral databases for repeating calculations. By providing database parameter when running MARFA executable, it is easy to switch between different databases and with that make a comparative analysis. In the next releases we plan to introduce support of the near coming HITRAN 2024 database.

4.2.2. Total Internal Partition Sums (TIPS)

Total internal partition sums (TIPS) are needed to determine temperature-dependent spectral line intensities. In MARFA, TIPS data are set in an external file and are implemented based on the study by Gamache, Farese, and Renaud [73]. We have introduced only partial data covering the first 74 isotopologues for the first 12 molecules (based on HITRAN ID and isotopologue local ID), over a temperature range of 20–1000 K. The TIPS values for a given isotopologue as a function of temperature can be accessed via the function TIPSofT in the Spectroscopy.f90 module. Future releases will incorporate more recent data from Gamache et al. [74], for more broad range of molecules and with considerations for reorganizing the input structure using Fortran subroutine or Python module.

4.2.3. Molecular Weights

Molecular weights are used for calculating Doppler half-widths and are stored in the MolarMasses.f90 module for the variety of isotopologues.

4.3. Quick start instructions

The process involves cloning the repository, building the project using the `fpm` build command, and installing the required Python packages. Predefined atmospheric profiles, such as `VenusCO2.dat` — which models the CO₂ distribution in Venus’s nightside atmosphere — are available for use. Currently, these profiles are limited to Venus constituents; alternatively, users may create custom atmospheric profiles following the specified format detailed in the project documentation [22].

Absorption coefficients are computed by executing the `fpm run` command with command line arguments that include the molecule title, spectral interval, line cut-off condition, atmospheric profile file, and other parameters. Post-processing is performed using an interactive provided Python script. Upon using it, a user is able to convert binary look-up table into human-readable format and to generate plot with dynamically adjusted title.

4.4. Scope of application and limitations

The codes are particularly well-suited for modeling absorption features in environments where both spectral and atmospheric parameters are uncertain. Our initial focus was made on Venus atmosphere, which explains current absence of predefined atmospheric profiles for other planets. The major scenario targeted by MARFA’s eleven-grid interpolation technique involves handling large cut-offs of spectral lines when continuum absorption function is missing. For that reason, currently MARFA does not support the incorporation of continuum absorption.

Currently preprocessed spectral databases only for the first 12 molecules (based on HITRAN ID) are available out of the box. This is a temporary limitation and it is due to the large size of these databases, making it impractical to store them in the repository. For details on how to generate spectra for additional molecules, refer to subsection 4.2.1.. Only cross-sections or volume absorption coefficients can be calculated when running current version of MARFA and it does not include functionality for modeling instrumental effects. Another limitation is the absence of support of the microwave region. It is planned to be added later, by making specific adjustments, such as Clough correction [75] to the van Vleck-Weisskopf (or van Vleck-Huber) theory [76] and handling “negative wavenumbers”.

4.5. Web application marfa.app

A web interface accessible at marfa.app has been developed enabling an immediate interaction with MARFA atmospheric absorption calculator. The example images 3, 4 and 5 illustrate essential parts of the application. We consider marfa.app as a good sketch of an atmospheric spectroscopy calculation lab/platform, build with well-established, modern, scalable and robust web stack. It may be an example of how to improve, transform and scale in near future existing more rich-functional solutions, like hitran.iao.ru [9]. Moreover marfa.app is lightweight and has an easy interface and could be used with ease in educational purposes. Web architecture of the marfa application allows to deploy it on any other hosting in without any issues. The source code is public and hosted on the dedicated repository [10], and like the MARFA source code it can be freely contributed and distributed under provided licenses.

The client side is built using the Next.js framework [77], which supports quick server-side rendering. On the server side, Django [78] and Django Rest Framework [79] backend frameworks are used, which are well-known and are highly scalable. They provide robust built-in database support mechanisms and functionality for building Web APIs (REST API is our primary choice). For the HTTP web server, Nginx [80] is used and PostgreSQL [81] is used as a primary database for storing information about users requests.

Integration between the backend and MARFA calculation kernel is achieved by leveraging Django's ViewSet to invoke external processes via Python's subprocess module [82]. This was chosen instead of f2py module from the Numpy [69], because there was a need to separate Fortran and Python layers of the application. Upon completion, the Fortran code generates the resulting PT-tables files, which are stored on the server. After processing of these files is complete, they are provided to a user with download links. Frontend and backend parts of the application are hosted within docker [83] containers, and a CI/CD pipeline based on GitHub Actions [84] is incorporated for automatic deployments.

Figure 3: Interface for setting parameters

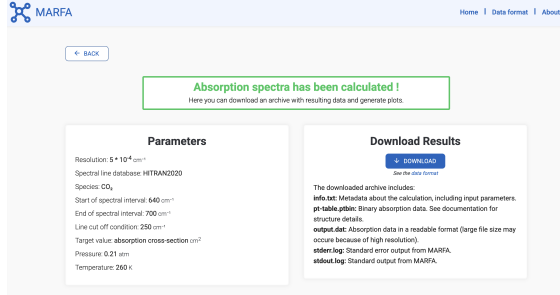


Figure 4: Interface for download options

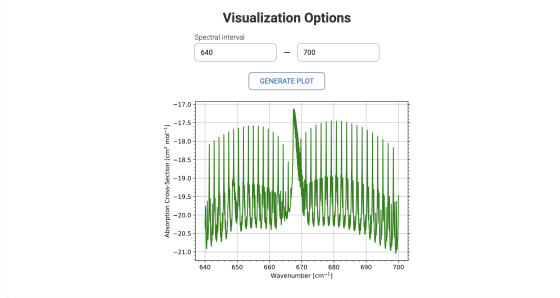


Figure 5: Interface for plot generation

5. Conclusion

MARFA (Molecular atmospheric Absorption with Rapid and Flexible Analysis) addresses critical challenges in calculation of molecular absorption in planetary atmospheres under sparse spectroscopic and atmospheric data conditions. By implementing an eleven-grid interpolation technique [6], MARFA can efficiently process large line cut-offs (500 cm^{-1} and beyond) and maintain high spectral resolution ($\approx 5 \times 10^{-4} \text{ cm}^{-1}$). This approach significantly reduces computational costs and makes it suitable for planetary conditions like Venus, where continuum functions remain poorly characterized on large spectral intervals.

The MARFA tool was tested using Venus as a benchmark, addressing challenges such as high-temperature CO₂ absorption, uncertain atmospheric profiles, uncertain line data and the need for extensive line-wing corrections. MARFA's features govern the ability to rapidly recalculate absorption spectra under varying parameters, which can make it valuable in diverse scenarios from Venusian conditions to exoplanetary analogs.

Provided not only as source code but also with a companion web interface (marfa.app), MARFA lowers the barrier to entry for educational and exploratory use. Because of its code design, effectiveness, flexibility and open-source commitment, MARFA project (source code + web application) can be a valuable resource for:

1. *Atmospheric spectroscopy research*: fast and accurate calculation of molecular spectra for radiative transfer models, general circulation models and in other frameworks; providing sensitivity analyses.
2. *Educational outreach*: teaching molecular spectroscopy and modern Fortran programming.
3. *Community-driven development*: transparent issue tracking and ease of installation and local development invite contributions from both scientific and IT-communities.

Future directions

Future improvements of MARFA are planned to be made by the authors of this study and by merge requests approvals of the independent contributions from the community. Planned improvements are tracked on the issues page, aiming to make it clear for contributors what is the current state of the project and what are the directions of improvements. Key focus areas are:

1. *Community-driven development*: Actively seeking for a feedback from researchers to test MARFA in novel scenarios; we hope that community input will guide us to prioritize new features.
2. *Performance Optimizations*:
 - Parallelizing spectral calculations across atmospheric levels using OpenMP [85] (inspired by Schreier et al. [71])
 - Reducing I/O bottlenecks in line-by-line processing through optimizing nested DO loops.
 - Introducing dynamic or user-defined spectral resolution.
3. *Data expansion*:
 - Integration and support of the HITRAN 2024 database and custom spectroscopic datasets (e.g., high-temperature CO₂ profiles). This may also include initializing a data storage for spectral databases preprocessed for MARFA calculations.
 - Enhancing TIPS datasets support.
 - Expanding the set of predefined atmospheric profiles (e.g. for Mars, Titan).
4. *Codebase Modernization*:
 - Refactoring legacy module LineGridCalc.f90 to adhere to the modern Fortran standards. We also consider converting this module, containing implementation of the interpolation method [6] to the Python package.
 - Resolving bugs identified through testing.
5. *New Features*:
 - Adding apparatus function convolution for instrumental response simulations.
 - Incorporating support of continuum absorption functions .
 - Extending MARFA support to microwave regimes.
6. *Web platform*: Improvements and scaling of the web platform relied on the needs of researchers and educational collectives.

Appendix A: Structure of the output PT-table file

The output PT-table files are generated and stored within the output/ptTables directory. Each PT-table file is a binary file and corresponds to a specific atmospheric level on which absorption was calculated. File name convention features only the level number, e.g. 1_.ptbin or 65_.ptbin. All the output files have the extension .ptbin.

The structure of the output file is organized into records that contain high-resolution absorption data (direct access file). Each record follows the structure outlined below:

Absorption data and resolution

Each record stores an array, which contains either the cross-section or absorption coefficient data for a specific wavenumber range. Each record corresponds to a 10 cm^{-1} -length interval, controlled by the `deltaWV` parameter in the source code. The finest grid in the interpolation technique [6] contains $NT = 20481$ nodes, thus defining the resolution of the output data:

$$\delta\nu = \frac{\text{deltaWV}}{NT-1} = \frac{10}{20480} \approx 5 \times 10^{-4} \text{ cm}^{-1}$$

Record Indexing

The relationship between a given wavenumber ν and the record number is defined as:

$$\text{recNum} = \text{int}\left(\frac{\nu}{10}\right)$$

For example, if absorption data for 7564 cm^{-1} is required, the corresponding record would be the 756th entry. For more details we address readers to the documentation [22], where additionally a code snippet is provided to extract data from the PT-table.

Appendix B: Utility for processing .par files

MARFA requires spectral database files to be in a specific format. These files should be placed in the data/databases directory and are typically created based on .par files from sources such as the HITRAN database. These .par files need to be preprocessed into required format before running the main executable. For users convenience, the utility provided in the codebase allows users to perform this preprocessing with simple command, and placing generated files in a required directory. For more details, please refer to the spectra databases section in the documentation [22].

Database file structure

Each spectral database file is a binary file which is organized as a collection of records (like the output PT-table file). Each record corresponds to one spectral line and contains its “core” parameters. The parameters include (for more details for each item, see HITRAN Database [23]):

1. the wavenumber of the transition (ν_{ij}) in double precision
2. the spectral line intensity (S_{ij}) at 296 K
3. the air-broadened half width at half maximum (HWHM) at 296 K (γ_{air})
4. the self-broadened half width at half maximum (HWHM) at 296 K (γ_{self})

5. the lower-state energy of the transition (E'')
6. the coefficient of the temperature dependence of the air-broadened half width (n_{air})
7. jointMolIso - custom parameter, which contains information on both molecule id (Mol) and isotopologue id (Iso). For more details, refer to the documentation.
8. the pressure shift at 296 K and 1 atm of the line position with respect to the vacuum transition wavenumber (δ_{air})

Since there are 8 parameters and for storing transition wavenumber one 8 bytes are needed, the total record length equals to $7 \times 4 + 8 = 36$ bytes.

Appendix C: Implementation of Voigt function

The approach we follow to compute the Voigt function is based on Humlicek [18] and Kuntz's [19] works. Original Kuntz's study optimizes Humlicek's method in two ways. Firstly, it rewrites complex rational approximations as real arithmetic operations, removing imaginary part computations unnecessary in applications, thus reducing floating-point operations. Secondly, it introduces recursive algorithm that leverages sorted x-grids to process subintervals collectively, reducing per-point region checks.

To summarize, our implementation incorporates the Kuntz's approach but with several modifications:

1. For $x > 15$, we substitute Voigt function with Lorentzian wing (optionally corrected with χ -factor) without fall in accuracy.
2. Kuntz's rational approximations are adopted for regions 1-3 (see fig.1 and Appendix in [19]).
3. Region 4 boundaries in (x, y) -plane are slightly changed and are set to: $\{y < 0.02, 1 < x < 5.5\}$ for an optimal speed-accuracy trade-off. Due to the Voigt function converging to Lorentzian for large x , we found it more convenient to use direct analytical asymptotic expressions instead of cumbersome polynomials (see pp. 823-824 in [19]), maintaining relative errors below 1%.
4. Recursive subdivision algorithm is omitted in favor of direct `if-else` blocks for region detection per (x, y) pair. We found it preferable to use simple and reliable `if-else` blocks instead of recursion due to the high vectorization capabilities of modern CPUs.

Below there is a demonstration of one of the asymptotics we use in region 4.

$$K(x, y) = \frac{y}{\pi} \int_{-\infty}^{+\infty} e^{-t^2} \phi(t), \quad \text{where} \quad \phi(t) = \frac{1}{(x-t)^2 + y^2} \quad (11)$$

is a function that varies significantly on a characteristic scale of y and $y \ll 1$.

To get analytical approximation, Taylor expansion to the second order term is applied:

$$\frac{\pi}{y} K(x, y) = \phi(0) \int_{-\infty}^{+\infty} e^{-t^2} dt + \frac{\partial \phi}{\partial t} \int_{-\infty}^{+\infty} e^{-t^2} t dt + \frac{\partial^2 \phi}{\partial t^2} \int_{-\infty}^{+\infty} e^{-t^2} t^2 dt \quad (12)$$

In the expression 12, first integral is $\sqrt{\pi}$, second integral is zero, while third one equals to $\frac{1}{2} \Gamma(\frac{3}{2}) = \frac{\sqrt{\pi}}{4}$. After passing values and derivatives of $\phi(t)$ to the 11 and 7, we get the asymptotic expression for the Voigt function:

$$f_V \approx f_L \cdot \left(1 + \frac{3}{2x^2}\right). \quad (13)$$

References

- [1] S. Roland Drayson. “Atmospheric Transmission in the CO₂ Bands Between 12 μ and 18 μ ”. In: *Appl. Opt.* 5 (3 1966), p. 385. DOI: 10.1364/AO.5.000385.
- [2] Shepard A Clough, Michael J Iacono, and Jean-Luc Moncet. “Line-by-line calculations of atmospheric fluxes and cooling rates: Application to water vapor”. In: *Journal of Geophysical Research: Atmospheres* 97.D14 (1992), pp. 15761–15785.
- [3] S. A. Clough et al. “Atmospheric radiative transfer modeling: A summary of the AER codes”. In: *Journal of Quantitative Spectroscopy and Radiative Transfer* 91 (2 Mar. 2005), pp. 233–244. ISSN: 00224073. DOI: 10.1016/j.jqsrt.2004.05.058.
- [4] Rainer Haus and Gabriele Arnold. “Radiative transfer in the atmosphere of Venus and application to surface emissivity retrieval from VIRTIS/VEX measurements”. In: *Planetary and Space Science* 58 (12 2010), pp. 1578–1598. ISSN: 00320633. DOI: 10.1016/j.pss.2010.08.001.
- [5] R. Haus, D. Kappel, and G. Arnold. “Radiative heating and cooling in the middle and lower atmosphere of Venus and responses to atmospheric and spectroscopic parameter variations”. In: *Planetary and Space Science* 117 (2015), pp. 262–294. ISSN: 00320633. DOI: 10.1016/j.pss.2015.06.024.
- [6] B.A. Fomin. “Effective interpolation technique for line-by-line calculations of radiation absorption in gases”. In: *Journal of Quantitative Spectroscopy and Radiative Transfer* 53.6 (1995), pp. 663–669.
- [7] B. A. Fomin. “Efficient line-by-line technique for calculating accurate and compact spectral lookup tables for satellite remote sensing”. In: *International Journal of Remote Sensing* 42 (8 2020), pp. 3074–3089. ISSN: 13665901. DOI: 10.1080/01431161.2020.1865586.
- [8] Martin Kuntz and Michael Höpfner. “Efficient line-by-line calculation of absorption coefficients”. In: *Radiative Transfer* 63 (1999), pp. 97–114.
- [9] HITRAN Team. *HITRAN On the WEB*. Accessed: 2025-01-25. 2025. URL: <https://hitran.iao.ru/>.
- [10] Razumovskyy. *MARFA WebApp*. <https://github.com/Razumovskyy/MARFA-webapp>. Accessed: 2025-01-25. 2025.
- [11] RM Goody and YL Yung. *Atmospheric Radiation: Theoretical Basis*. Oxford University Press, 1989.
- [12] I. E. Gordon et al. “The HITRAN2020 molecular spectroscopic database”. In: *Journal of Quantitative Spectroscopy and Radiative Transfer* 277 (Jan. 2022). ISSN: 00224073. DOI: 10.1016/j.jqsrt.2021.107949.
- [13] I. E. Gordon et al. “The HITRAN2016 molecular spectroscopic database”. In: *Journal of Quantitative Spectroscopy and Radiative Transfer* 203 (Dec. 2017), pp. 3–69. ISSN: 00224073. DOI: 10.1016/j.jqsrt.2017.06.038.
- [14] L. S. Rothman et al. “HITEMP, the high-temperature molecular spectroscopic database”. In: *Journal of Quantitative Spectroscopy and Radiative Transfer* 111 (15 Oct. 2010), pp. 2139–2150. ISSN: 00224073. DOI: 10.1016/j.jqsrt.2010.05.001.
- [15] Nicole Jacquinet-Husson et al. “The 2003 edition of the GEISA/IASI spectroscopic database”. In: *Journal of Quantitative Spectroscopy and Radiative Transfer* 95 (4 Nov. 2005), pp. 429–467. ISSN: 00224073. DOI: 10.1016/j.jqsrt.2004.12.004.
- [16] N. Jacquinet-Husson et al. “The GEISA spectroscopic database: Current and future archive for Earth and planetary atmosphere studies”. In: *Journal of Quantitative Spectroscopy and Radiative Transfer* 109 (6 Apr. 2008), pp. 1043–1059. ISSN: 00224073. DOI: 10.1016/j.jqsrt.2007.12.015.
- [17] BH Armstrong. “Spectrum line profiles: the Voigt function”. In: *Journal of Quantitative Spectroscopy and Radiative Transfer* 7.1 (1967), pp. 61–88.
- [18] Josef Humlíček. “Optimized computation of the Voigt and complex probability functions”. In: *Journal of Quantitative Spectroscopy and Radiative Transfer* 27.4 (1982), pp. 437–444.
- [19] M. Kuntz. “A new implementation of the Humlíček algorithm for the calculation of the Voigt profile function”. In: *Journal of Quantitative Spectroscopy and Radiative Transfer* 57.6 (1997), pp. 819–824.
- [20] Lazaros Oreopoulos et al. “The continual intercomparison of radiation codes: Results from phase I”. In: *Journal of Geophysical Research: Atmospheres* 117.D6 (2012).

[21] Rangasayi N Halthore et al. “Intercomparison of shortwave radiative transfer codes and measurements”. In: *Journal of Geophysical Research: Atmospheres* 110.D11 (2005).

[22] Razumovskyy. MARFA. <https://github.com/Razumovskyy/MARFA>. Accessed: 2024-02-01. 2024.

[23] HITRAN Database. *Definitions and Units for HITRAN Data*. <https://hitran.org/docs/definitions-and-units/>. Accessed: October 29, 2024. 2024.

[24] H. Tran, N. H. Ngo, and J. M. Hartmann. “Efficient computation of some speed-dependent isolated line profiles”. In: *Journal of Quantitative Spectroscopy and Radiative Transfer* 129 (Nov. 2013), pp. 199–203. ISSN: 00224073. DOI: 10.1016/j.jqsrt.2013.06.015.

[25] N. H. Ngo et al. “An isolated line-shape model to go beyond the Voigt profile in spectroscopic databases and radiative transfer codes”. In: *Journal of Quantitative Spectroscopy and Radiative Transfer* 129 (Nov. 2013), pp. 89–100. ISSN: 00224073. DOI: 10.1016/j.jqsrt.2013.05.034.

[26] PW Rosenkranz. “Pressure broadening of rotational bands. I. A statistical theory”. In: *The Journal of chemical physics* 83.12 (1985), pp. 6139–6144.

[27] Philip L. Varghese and Ronald K. Hanson. “Collisional narrowing effects on spectral line shapes measured at high resolution”. In: *Applied Optics* 23 (1984), pp. 2376–2385.

[28] Darrell E. Burch et al. “Absorption of infrared radiant energy by CO₂ and H₂O. IV. Shapes of collision-broadened CO₂ lines”. In: *JOSA* 59.3 (1969), pp. 267–280.

[29] James B. Pollack et al. “Near-Infrared Light from Venus’ Nightside: A Spectroscopic Analysis”. In: *Icarus* 103 (1 1993), pp. 1–42. ISSN: 10902643. DOI: 10.1006/icar.1993.1055.

[30] SA Clough, FX Kneizys, and RW Davies. “Line Shape and the Water Vapor Continuum”. In: *Atmospheric Research* 23 (1989), pp. 229–241.

[31] MV Tonkov et al. “Measurements and empirical modeling of pure CO₂ absorption in the 2.3- μ m region at room temperature: far wings, allowed and collision-induced bands”. In: *Applied optics* 35.24 (1996), pp. 4863–4870.

[32] MY Perrin and JM Hartmann. “Temperature-dependent measurements and modeling of absorption by CO₂-N₂ mixtures in the far line-wings of the 4.3 μ m CO₂ band”. In: *Journal of Quantitative Spectroscopy and Radiative Transfer* 42.4 (1989), pp. 311–317.

[33] DP Edwards. “Atmospheric transmittance and radiance calculations using line-by-line computer models”. In: 1988, pp. 94–116. DOI: 10.1117/12.975622. URL: <http://proceedings.spiedigitallibrary.org/pdfaccess.ashx?url=/data/conferences/spiep/89574/>.

[34] Robert West, David Crisp, and Luke Chen. “Mapping transformations for broadband atmospheric radiation calculations”. In: *Journal of Quantitative Spectroscopy and Radiative Transfer* 43.3 (1990), pp. 191–199.

[35] Larry L. Gordley, Benjamin T. Marshall, and D. Allen Chu. “LINEPAK: Algorithms for Modeling Spectral Transmittance and Radiance”. In: *J. Quant. Spectrosc. Radiat. Transfer* 52 (5 1994), pp. 563–580.

[36] Lawrence Sparks. “Efficient line-by-line calculation of absorption coefficients to high numerical accuracy”. In: *Journal of Quantitative Spectroscopy and Radiative Transfer* 57.5 (1997), pp. 631–650.

[37] DV Titov and Rainer Haus. “A fast and accurate method of calculation of gaseous transmission functions in planetary atmospheres”. In: *Planetary and space science* 45.3 (1997), pp. 369–377.

[38] Michel Kruglanski and Martine De Maziere. “Fast method for calculating infrared spectral transmittances in the wings of absorption lines”. In: *Journal of quantitative spectroscopy and radiative transfer* 94.1 (2005), pp. 117–125.

[39] Franz Schreier. “Optimized evaluation of a large sum of functions using a three-grid approach”. In: *Computer Physics Communications* 174 (10 May 2006), pp. 783–792. ISSN: 00104655. DOI: 10.1016/j.cpc.2005.12.015.

[40] Roman V Kochanov et al. “HITRAN Application Programming Interface (HAPI): A comprehensive approach to working with spectroscopic data”. In: *Journal of Quantitative Spectroscopy and Radiative Transfer* 177 (2016), pp. 15–30.

[41] Boris Fomin and Mikhail Razumovskiy. “Effective parameterization of absorption by gaseous species and unknown UV absorber in 125–400 nm region of Venus atmosphere”. In: *Journal of Quantitative Spectroscopy and Radiative Transfer* 286 (2022), p. 108201. ISSN: 00224073. DOI: 10.1016/j.jqsrt.2022.108201.

[42] D. Ehrenreich et al. “Transmission spectrum of Venus as a transiting exoplanet”. In: *Astronomy and Astrophysics* 537 (2012). ISSN: 00046361. DOI: 10.1051/0004-6361/201118400.

[43] Laura Schaefer and Bruce Fegley. “Atmospheric chemistry of VENUS-like exoplanets”. In: *Astrophysical Journal* 729 (1 Mar. 2011). ISSN: 15384357. DOI: 10.1088/0004-637X/729/1/6.

[44] L. V. Zasova et al. “Structure of the Venusian atmosphere from surface up to 100 km”. In: *Cosmic Research* 44.4 (2006), pp. 364–383. DOI: 10.1134/S0010952506040095.

[45] A. Seiff et al. “Models of the structure of the atmosphere of Venus from the surface to 100 kilometers altitude”. In: *Advances in Space Research* 5 (11 1985), pp. 3–58. ISSN: 02731177. DOI: 10.1016/0273-1177(85)90197-8.

[46] GM Keating, JY Nicholson III, and LR Lake. “Venus upper atmosphere structure”. In: *Journal of Geophysical Research: Space Physics* 85.A13 (1980), pp. 7941–7956.

[47] GM Keating et al. “Models of Venus neutral upper atmosphere: Structure and composition”. In: *Advances in Space Research* 5.11 (1985), pp. 117–171.

[48] A Seiff and Donn B Kirk. “Structure of the Venus mesosphere and lower thermosphere from measurements during entry of the Pioneer Venus probes”. In: *Icarus* 49.1 (1982), pp. 49–70.

[49] Constantine C.C. Tsang et al. “Tropospheric carbon monoxide concentrations and variability on Venus from Venus Express/VIRTIS-M observations”. In: *Journal of Geophysical Research E: Planets* 114.5 (2009), pp. 1–13. DOI: 10.1029/2008JE003089.

[50] Rainer Haus, David Kappel, and Gabriele Arnold. “Self-consistent retrieval of temperature profiles and cloud structure in the northern hemisphere of Venus using VIRTIS/VEX and PMV/VENERA-15 radiation measurements”. In: *Planetary and Space Science* 89 (2013), pp. 77–101.

[51] C. C.C. Tsang et al. “A correlated-k model of radiative transfer in the near-infrared windows of Venus”. In: *Journal of Quantitative Spectroscopy and Radiative Transfer* 109.6 (2008), pp. 1118–1135. DOI: 10.1016/j.jqsrt.2007.12.008.

[52] Laurence S Rothman et al. “The HITRAN 2004 molecular spectroscopic database”. In: *Journal of quantitative spectroscopy and radiative transfer* 96.2 (2005), pp. 139–204.

[53] Laurence S Rothman et al. “The HITRAN 2008 molecular spectroscopic database”. In: *Journal of Quantitative Spectroscopy and Radiative Transfer* 110.9-10 (2009), pp. 533–572.

[54] L. S. Rothman et al. “The HITRAN2012 molecular spectroscopic database”. In: *Journal of Quantitative Spectroscopy and Radiative Transfer* 130 (Nov. 2013), pp. 4–50. ISSN: 00224073. DOI: 10.1016/j.jqsrt.2013.07.002.

[55] Laurence S Rothman et al. “HITRAN HAWKS and HITEMP: high-temperature molecular database”. In: *Atmospheric Propagation and Remote Sensing IV* 2471 (1995), pp. 105–111.

[56] Sergey A. Tashkun et al. “CDSD-1000, the high-temperature carbon dioxide spectroscopic databank”. In: *Journal of Quantitative Spectroscopy and Radiative Transfer* 82.1-4 (2003), pp. 165–196.

[57] David Kappel et al. “Refinements in the data analysis of VIRTIS-M-IR Venus nightside spectra”. In: *Advances in Space Research* 50 (2 July 2012), pp. 228–255. ISSN: 02731177. DOI: 10.1016/j.asr.2012.03.029.

[58] David Kappel, Gabriele Arnold, and Rainer Haus. “Multi-spectrum retrieval of Venus IR surface emissivity maps from VIRTIS/VEX nightside measurements at Themis Regio”. In: *Icarus* 265 (Feb. 2016), pp. 42–62. ISSN: 10902643. DOI: 10.1016/j.icarus.2015.10.014.

[59] Bruno Bézard et al. “Water vapor abundance near the surface of Venus from Venus Express/VIRTIS observations”. In: *Journal of Geophysical Research: Planets* 114 (5 2009). ISSN: 01480227. DOI: 10.1029/2008JE003251.

[60] Bruno Bézard et al. “The 1.10- and 1.18- μ m nightside windows of Venus observed by SPICAV-IR aboard Venus Express”. In: *Icarus* 216 (1 2011), pp. 173–183. ISSN: 00191035. DOI: 10.1016/j.icarus.2011.08.025.

[61] M Fukabori, T Nakazawa, and M Tanaka. “Absorption properties of infrared active gases at high pressures—I. CO₂”. In: *Journal of Quantitative Spectroscopy and Radiative Transfer* 36.3 (1986), pp. 265–270.

[62] Bruno Bézard et al. “The deep atmosphere of Venus revealed by high-resolution nightside spectra”. In: *Nature* 345.6275 (1990), pp. 508–511.

[63] Bruno Bézard et al. “Water vapor abundance near the surface of Venus from Venus Express/VIRTIS observations”. In: *Journal of Geophysical Research: Planets* 114.E5 (2009).

[64] Sergey Korkin et al. “A practical guide to coding line-by-line trace gas absorption in Earth’s atmosphere”. In: *Journal of Quantitative Spectroscopy and Radiative Transfer* (2025), p. 109345.

[65] Fortran-lang Contributors. *fpm: Fortran Package Manager*. <https://fortran-lang.org/fpm/>. Accessed: 2024-04-27. 2024.

[66] Michael Metcalf et al. *Modern Fortran Explained: Incorporating Fortran 2023*. Oxford University Press, 2024.

[67] ISO/IEC JTC1/SC22/WG5. *Fortran 2023 standard*. <https://wg5-fortran.org/f2023.html>. Accessed: 2024-04-27. 2023.

[68] Franz Schreier. “The Voigt and complex error function: Humlíček’s rational approximation generalized”. In: *Monthly Notices of the Royal Astronomical Society* 479.3 (2018), pp. 3068–3075.

[69] Charles R Harris et al. “Array programming with NumPy”. In: *Nature* 585.7825 (2020), pp. 357–362.

[70] Franz Schreier et al. “Py4cats—PYthon for computational ATmospheric spectroscopy”. In: *Atmosphere* 10.5 (2019), p. 262.

[71] Franz Schreier et al. “GARLIC - A general purpose atmospheric radiative transfer line-by-line infrared-microwave code: Implementation and evaluation”. In: *Journal of Quantitative Spectroscopy and Radiative Transfer* 137 (2014), pp. 29–50. ISSN: 00224073. DOI: 10.1016/j.jqsrt.2013.11.018.

[72] Salvatore Larosa et al. “PyRTlib: an educational Python-based library for non-scattering atmospheric microwave radiative transfer computations”. In: *Geoscientific Model Development* 17.5 (2024), pp. 2053–2076.

[73] Robert R. Gamache, Michaella Farese, and Candice L. Renaud. “A spectral line list for water isotopologues in the 1100–4100 cm⁻¹ region for application to CO₂-rich planetary atmospheres”. In: *Journal of Molecular Spectroscopy* 326 (Aug. 2016), pp. 144–150. ISSN: 1096083X. DOI: 10.1016/j.jms.2015.09.001.

[74] Robert R. Gamache et al. “Total internal partition sums for the HITRAN2020 database”. In: *Journal of Quantitative Spectroscopy and Radiative Transfer* 271 (Sept. 2021). ISSN: 00224073. DOI: 10.1016/j.jqsrt.2021.107713.

[75] SA Clough et al. *Atmospheric Water Vapor, chapter 2*. 1980.

[76] J. H. Van Vleck and D. L. Huber. “Absorption, emission, and linebreadths: A semihistorical perspective”. In: *Reviews of Modern Physics* 49 (4 1977), pp. 939–959. ISSN: 00346861. DOI: 10.1103/RevModPhys.49.939.

[77] Vercel. *Next.js*. <https://nextjs.org/>. Accessed: October 29, 2024. 2024.

[78] Django Software Foundation. *Django*. <https://www.djangoproject.com/>. Accessed: October 29, 2024. 2024.

[79] Tom Christie. *Django REST Framework*. <https://www.django-rest-framework.org/>. Accessed: October 29, 2024. 2024.

[80] Igor Sysoev and Inc. Nginx. *Nginx: A High-Performance Web Server and Reverse Proxy Server*. <https://nginx.org/>. Accessed: October 29, 2024. 2024.

[81] PostgreSQL Global Development Group. *PostgreSQL: The World’s Most Advanced Open Source Relational Database*. <https://www.postgresql.org/>. Accessed: October 29, 2024. 2024.

[82] Python Software Foundation. *subprocess — Subprocess management*. 3.11. Accessed: October 29, 2024. Python. 2024. URL: <https://docs.python.org/3/library/subprocess.html>.

[83] Inc. Docker. *Docker: Empowering App Development for Developers and Enterprises*. <https://www.docker.com/>. Accessed: 2025-01-25. 2025.

- [84] Inc. GitHub. *GitHub Actions: Automate Your Workflow from Idea to Production*. <https://github.com/features/actions>. Accessed: 2025-01-25. 2025.
- [85] OpenMP Architecture Review Board. *OpenMP Application Programming Interface*. Version 5.2. 2023. URL: <https://www.openmp.org/specifications/>.